Hindawi
Mathematical Problems in Engineering
Volume 2018, Article ID 4341825, 9 pages
https://doi.org/10.1155/2018/4341825

Research Article

Improved Model-Free Adaptive Sliding-Mode-Constrained Control for Linear Induction Motor considering End Effects

Xiaoqi Song,[1] Dezhi Xu ,[1] Weilin Yang,[1] Yan Xia,[1] and Bin Jiang [2]

[1]*School of Internet of Things Engineering, Jiangnan University, Wuxi 214122, China*
[2]*College of Automation Engineering, Nanjing University of Aeronautics and Astronautics, Nanjing 211106, China*

Correspondence should be addressed to Dezhi Xu; xudezhi@jiangnan.edu.cn

Received 5 February 2018; Accepted 29 April 2018; Published 29 May 2018

Academic Editor: Tarek Ahmed-Ali

As a kind of special motors, linear induction motors (LIM) have been an important research field for researchers. However, it gives a great velocity control challenge due to the complex nonlinearity, high coupling, and unique end effects. In this article, an improved model-free adaptive sliding-mode-constrained control method is proposed to deal with this problem dispensing with internal parameters of the LIM. Firstly, an improved compact form dynamic linearization (CFDL) technique is used to simplify the LIM plant. Besides, an antiwindup compensator is applied to handle the problem of the actuator under saturations in case during the controller design. Furthermore, the stability of the closed system is proved by Lyapunov stability method theoretically. Finally, simulation results are given to demonstrate that the proposed controller has excellent dynamic performance and stronger robustness compared with traditional PID controller.

1. Introduction

In the past few decades, the LIM has been widely used in many fields, such as military, household appliances, industrial automation, and transportation [1–4]. Compared with the conventional rotary induction motors (RIM), the main advantages of LIM are as follows: (1) it does not have any converter, gear, or other intermediate conversion mechanism which can reduce mechanical loss; (2) it is only driven by magnetic force which makes the LIM have the features of high speed and low noise [5, 6]. Even though the driving principle of a LIM is similar to that of a RIM, the parameters of LIM are time-varying, such as end effects, slip frequency, dynamic air gap, three-phase imbalance, and track structure [7–9]. Among them, the end effects greatly affect the LIM control performance, and the faster the speed, the more significant the impact. Therefore, during the modeling of the LIM, the end effects must be considered.

With the quick development of science and technology, many model-based control methods are proposed to handle LIM control problems. In [10], an adaptive backstepping method is proposed to deal with the position tracking problem of the LIM. In [11], an optimized adaptive tracking control is applied for a LIM considering the uncertainties. In [12], the authors use input-output feedback linearization control technique with online model reference adaptive system (MRAS) method suiting the induction resistance to realize the velocity following goal, whereas the three mentioned methods are highly dependent on the accuracy of the model. Once the model is improperly defined or the system parameters cannot be accurately obtained, the dynamic response of the system will hardly be satisfied. Besides, some non-model-based control methods are also proposed for LIM control problems. In [13], the researchers present a real-time discrete neural control scheme based on a recurrent high order neural network trained online to a LIM. In [14, 15], some methods based on fuzzy control are also used to have the problem solved. However, even if we neglect the complexity of the selection of fuzzy rules and the uncertainty of the neural network nodes, these methods have not considered the input saturation problems which may result in system instability.

Model-free adaptive control (MFAC) was first proposed in 1994 and is a hot topic in the field of data-driven modeling [16–19]. It is a method that only relies on input/output (I/O) data and does not need any internal information of

the plant. The main design steps of the MFAC are divided into three categories: (1) using CFDL technique to transfer the nonlinear system into self-designed linear model based on a parameter called pseudo-partial-derivative (PPD), (2) estimating the value of the PPD through a variety of methods, and (3) devising the controller based on self-designed linear model. For now, MFAC has been widely applied in all kinds of fields, such as multiagent systems [20], chemical process [19, 21], and intelligent transportation [22]. Moreover, due to the fact that sliding-mode control (SMC) is designed without object parameters and disturbance, it gets the merits of quick response and high fitness. SMC is also a hot topic and is applied in a variety of fields [23, 24] and has been used in combination with MFAC firstly in [25].

In this paper, an improved CFDL technique is used to linearize the LIM model considering end effects based on PPD estimation algorithm. And we design a model-free adaptive constrained sliding-mode control for the system considering input saturations. So as to avoid the instability caused by saturations, we design an antiwindup compensator to make the output continue to follow the given reference.

The rest of this paper is organized as follows. Section 2 briefly introduces the model of the LIM considering end effects. In Section 3, the main results of the proposed control strategy are given. The simulation results are shown in Section 4 to verify the effectiveness and robustness of the method. Finally, some conclusions are drawn in Section 5.

2. Problem Formulation for LIM

Similar to a RIM, a LIM is made up of primary and secondary components as shown in Figure 1. Besides, a LIM is obtained by a RIM that is opened longitudinally in a transverse direction. However, the biggest difference between a LIM and a RIM is that the LIM contains end effects which are caused by its structure. The end effects can be explained as follows: when the primary moves, eddy current occurs in the corresponding secondary conductor plate at the outlet and inlet terminals, and the direction of flow is opposite to the primary current, so that the air gap magnetic field will be distorted [9, 11]. Researchers generally use a parameter Q to express this phenomenon as

$$Q = \frac{l \cdot R_r}{v \cdot L_r}, \tag{1}$$

where l denotes the primary length, v denotes the speed of a LIM, and L_r and R_r denote the secondary inductance and resistance, respectively.

When the LIM is in a stationary state, we can consider its equivalent circuit as a RIM. Nevertheless, when the LIM is in a motion state, the model of a LIM in synchronously rotating reference frame should be improved as follows [8, 11]:

$$\begin{aligned} V_{sd} &= R_s i_{sd} + p\phi_{sd} - \omega_e \phi_{sq} \\ V_{sq} &= R_s i_{sq} + p\phi_{sq} - \omega_e \phi_{sd} \\ V_{rd} &= R_r i_{rd} + p\phi_{rd} - (\omega_e - \omega_r)\phi_{rq} \end{aligned}$$

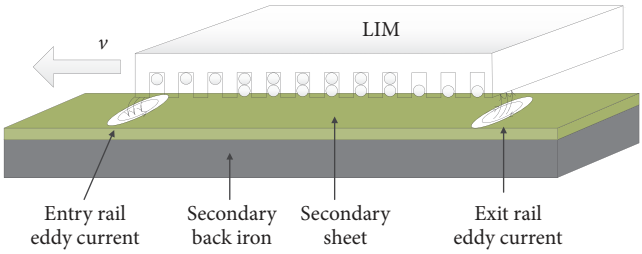

Figure 1: Structure of a LIM.

$$V_{rq} = R_r i_{rq} + p\phi_{rq} + (\omega_e - \omega_r)\phi_{rd}, \tag{2}$$

where (V_{sd}, V_{rd}), (i_{sd}, i_{rd}), and (ϕ_{sd}, ϕ_{rd}) denote the primary and secondary voltage, current, and flux linkage in d-axis; (V_{sq}, V_{rq}), (i_{sq}, i_{rq}), and (ϕ_{sq}, ϕ_{rq}) denote the corresponding parameters in q-axis; R_s denotes the primary resistance; ω_e and ω_r denote the angular frequency of stator and rotor; and p denotes the differential operator.

According to [8, 11], the flux linkage in dq-axis can be expressed as follows:

$$\begin{aligned} \phi_{sd} &= L_{sl} i_{sd} + L_m (1 - f(Q))(i_{sd} + i_{rd}) \\ \phi_{rq} &= L_{sl} i_{sq} + L_m (1 - f(Q))(i_{sq} + i_{rq}) \\ \phi_{rd} &= L_{rl} i_{rd} + L_m (1 - f(Q))(i_{sd} + i_{rd}) \\ \phi_{rq} &= L_{rl} i_{rq} + L_m (1 - f(Q))(i_{sq} + i_{rq}), \end{aligned} \tag{3}$$

where $f(Q) = (1 - e^{-Q})/Q$ is an important parameter during the process of modeling for a LIM, L_m is the magnetic inductance, and L_{sl} and L_{rl} are the primary and secondary leakage inductance. Meanwhile, the electromagnetic thrust force can be expressed as

$$F_{et} = K_f (\phi_{rd} \cdot i_{sq} - \phi_{rq} \cdot i_{sd}), \tag{4}$$

where $K_f = 3\pi P L_m/(2hL_r)$, P means the pole numbers, and h is the pole pitch.

By using the indirect vector control (IVC) technology, we can convert the linear induction motor model into a DC motor model which brings about great convenience to the control of the LIM. Thus, with IVC technology, orientate the rotor flux to the d-axis, and we get

$$\begin{aligned} \phi_{rq} &= \dot{\phi}_{rq} = 0 \\ V_{rd} &= V_{rq} = 0, \end{aligned} \tag{5}$$

where $\dot{\phi}_{rq}$ denotes the differential of ϕ_{rq}.

According to (2)–(5), the dynamic model of LIM considering end effects under IVC can be described as

$$\begin{aligned}
\frac{di_{sd}}{dt} &= -\frac{R_s}{L(Q)}i_{sd} + \frac{V_{sd}}{L(Q)} + \omega_e i_{sq} \\
\frac{di_{sq}}{dt} &= -\omega_e\left[i_{sd} + \frac{L_m(1-f(Q))}{L(Q)(L_r - L_m f(Q))}\phi_{dr}\right] \\
&\quad - \frac{R_s}{L(Q)}i_{sq} + \frac{V_{sq}}{L(Q)} \\
\frac{d\phi_{rd}}{dt} &= \frac{L_m[1-f(Q)]i_{sd} - \phi_{rd}}{T_r - L_m f(Q)/R_r} \\
\omega_{sl} &= \omega_e - \omega_r = \frac{L_m(1-f(Q))}{T_r - L_m f(Q)/R_r}\frac{i_{sq}}{\phi_{rd}} \\
F_{et} &= K_T i_{sq} = M\cdot\frac{dv}{dt} + D\cdot v + F_{\text{Load}},
\end{aligned} \tag{6}$$

where M denotes the total mass of the moving object, D denotes the viscosity coefficient, F_{Load} denotes the external force disturbance, ω_{sl} denotes the slip frequency, and

$$\begin{aligned}
L(Q) &= L_s - L_m f(Q) - \frac{[L_m(1-f(Q))]^2}{L_r - L_m f(Q)} \\
K_T &= \frac{3}{2}P\frac{\pi}{h}\frac{L_m(1-f(Q))}{L_r - L_m f(Q)}\phi_{dr} \\
T_r &= \frac{L_r}{R_r}
\end{aligned} \tag{7}$$

Besides, according to (6), the acceleration of LIM can be redescribed as

$$\frac{dv}{dt} = \frac{K_T}{M}i_{sq} + A\cdot v + B, \tag{8}$$

where $A = -D/M; B = -F_{\text{Load}}/M$.

Remark 1. Taking into account the physical characteristics of the inverter structure and the safety of the system, the input saturation conditions must be considered. The control inputs are limited to

$$\begin{aligned}
u_{qs\min} &\leqslant u_{qs} \leqslant u_{qs\max}; \\
\dot{u}_{qs\min} &\leqslant \dot{u}_{qs} \leqslant \dot{u}_{qs\max},
\end{aligned} \tag{9}$$

where $\dot{u}_{qs}$ denotes the differential of u_{qs} and $(u_{qs\min}, u_{qs\max})$ and $(\dot{u}_{qs\min}, \dot{u}_{qs\max})$ denote the lower and upper bound of u_{qs} and $\dot{u}_{qs}$.

As speed is the most important performance parameter of motor control, we choose the velocity as our main control objective. Then, the model of a LIM considering end effects can be described in the following discrete-time unknown Nonlinear AutoRegressive with eXogenous input (NARX) model

$$\begin{aligned}
x(t+1) = g(&x(t),\ldots,x(t-t_x),u(t),\ldots,u(t-t_u), \\
&d(t),\ldots,d(t-t_d)),
\end{aligned} \tag{10}$$

where system output x denotes the speed of the LIM v, input u denotes the primary voltage in q-axis u_{qs}, and disturbance d denotes the external force disturbance F_{Load}. And t_x, t_u, and t_d mean the unknown orders, and $g(\cdot)$ is the unknown function. Apparently, the LIM satisfies the following two basic assumptions.

Assumption 2. The partial derivatives of $g(\cdot)$ for $u(t)$ and $d(t)$ are continuous.

Assumption 3. The plant (10) satisfies the condition of generalised Lipschitz, that is to say, $\forall t$, $|\Delta u(t-1)| \neq 0$ and $|\Delta d(t-1)| \neq 0$, satisfying $\Delta x(t) \leqslant \Lambda_1|\Delta u(t-1)|$ and $\Delta x(t) \leqslant \Lambda_2|\Delta u(t-1)|$, where $\Delta x(t) = x(t) - x(t-1)$, $\Delta u(t) = u(t) - u(t-1)$, and $\Delta d(t) = d(t) - d(t-1)$, and Λ_1, Λ_2 are unknown constants.

Remark 4. For general nonlinear systems, Assumption 2 is a common condition in the process of controller design. And Assumption 3 is a constrained condition that limits the changes of the outputs of the plant caused by system inputs and disturbance.

3. Main Results

In this section, an improved model-free adaptive SMC scheme is proposed for the LIM through the CFDL technology. The main contributions of this section are as follows:

(1) Transferring the LIM system into a data-based CFDL model considering the disturbance.

(2) Proposing the PPD estimation algorithm based on observers.

(3) Designing the model-free adaptive integral sliding-model controller via an antiwindup compensator.

(4) Proving the stability of the closed-loop system by Lyapunov stability theory.

3.1. Data-Driven Modeling for LIM and PPD Estimation Algorithm. Data-driven modeling method was originally proposed by HOU [17, 18, 26], and it is totally divided into three forms: CFDL, partial form dynamic linearization (PFDL), and full-form dynamic linearization (FFDL). In this paper, the CFDL technique is used to linearize the LIM system. When $|\Delta u(t)| \neq 0$, we can obtain the data-driven model as

$$\Delta x(t+1) = \theta_1 \Delta u(t) + \theta_2 \Delta d(t), \tag{11}$$

where $\theta_1 \leqslant \Lambda_1$ and $\theta_2 \leqslant \Lambda_2$ are the PPDs of the system.

The process of the proof is the same as that of [27].

To describe the system more conveniently, model (11) can be rewritten as follows:

$$x(t+1) = x(t) + Z^T(t)\Phi(t), \tag{12}$$

where $Z(t) = [\Delta u(t), \Delta d(t)]^T$ and $\Phi(t) = [\theta_1(t), \theta_2(t)]^T$.

The system output identification observer can be designed as

$$\hat{x}(t+1) = \hat{x}(t) + Z^T(t)\,\widehat{\Phi}(t) + Me_e(t), \tag{13}$$

where $\hat{x}(t)$ and $\widehat{\Phi}(t)$ mean the estimated value of output and PPDs of the system at time t, $e_e(t) = x(t) - \hat{x}(t)$ denotes the estimation error of the system output, and the gain K is chosen in the unit cycle. According to (12) and (13), the dynamic of the estimation error $e_e(t)$ can be described as

$$e_e(t+1) = Z^T(t)\,\widetilde{\Phi}(t) + Ne_e(t), \tag{14}$$

where $N = 1-M$ and $\widetilde{\Phi}(t) = \Phi(t)-\widehat{\Phi}(t)$ means the estimation error of the PPDs. The adaptive update PPD algorithm is given by

$$\widehat{\Phi}(t+1) = \widehat{\Phi}(t) + Z(t)\,\Gamma(t)\left(e_e(t+1) - Ne_e(t)\right), \tag{15}$$

where the gain function is chosen as

$$\Gamma(t) = \frac{2}{\|Z(t)\|^2 + \partial} \tag{16}$$

Due to the fact that $\partial > 0$ is a chosen positive constant, it is for sure that $\Gamma(t)$ is positive. Besides, according to the practical assumption $\|Z(t)\| \leqslant \Omega$, $\Gamma(t)$ can be limited as

$$\Gamma(t) \geqslant \frac{2}{\Omega^2 + \partial} = \upsilon > 0 \tag{17}$$

In view of (14) and (15), the error dynamics of the system can be obtained as

$$\begin{aligned} e_e(t+1) &= Z^T(t)\,\widetilde{\Phi}(t) + Ne_e(t) \\ \widetilde{\Phi}(t+1) &= H\widetilde{\Phi}(t), \end{aligned} \tag{18}$$

where $H = I_{2\times2} - Z(t)\Gamma(t)Z^T(t)$ and $I_{2\times2}$ means the two-order unit matrix.

Theorem 5. *The equivalent of $[e_e, \widetilde{\Phi}]$ is globally uniformly stable. Furthermore, the estimation error of output $e_e(t)$ converges to 0; that is to say, $\lim_{t\to\infty}|e_e(t)| = 0$*

Proof. Consider the Lyapunov function as

$$V_A(t) = P_A {e_e}^2(t) + \lambda_A \widetilde{\Phi}^T(t)\,\widetilde{\Phi}(t), \tag{19}$$

where λ_A is a positive constant and P_A is also a positive constant figured by $P_A - F_A^2 P_A = Q_A$ with Q_A being a positive constant. Then, the difference of $V_A(t)$ can be written as

$$\begin{aligned} \Delta V_A(t) &= V_A(t+1) - V_A(t) \\ &= P_A Z^T(t)\,\widetilde{\Phi}(t)\,\widetilde{\Phi}^T(t)\,Z(t) \\ &\quad - 2P_A F_A Z^T(t)\,\widetilde{\Phi}(t)\,e_e(t) + P_A F_A^2 e_e^2(t) \\ &\quad + \widetilde{\Phi}^T(t)\left(\lambda_A H^T H - \lambda_A\right)\widetilde{\Phi}(t) + P_A e_e^2(t) \\ &= -\Theta_A^T(t)\left[\lambda_A\mu_A\Gamma^T(t)\,\Gamma(t) - P_A\right]\Theta_A(t) \\ &\quad - Q_A e_e^2(t) + 2P_A F_A e_e(t)\,\Theta_A(t) \\ &\leq -\left[\lambda_A\mu_A\Gamma^T(t)\,\Gamma(t) - P_A\right]\|\Theta_A(t)\|^2 \\ &\quad + 2P_A F_A |e_e(t)|\,\|\Theta_A(t)\| - Q_A |e_e(t)|^2 \\ &\leq -a_1 |e_e(t)|^2 - a_2 \|\Theta_A(t)\|^2, \end{aligned} \tag{20}$$

where $\Theta_A(t) = Z^T(t)\widetilde{\Phi}(t)$, $a_2 = \lambda_A\mu_A\upsilon^2 - P_A - \iota P_A^2 F_A^2$, and $a_1 = Q_A - (1/\iota)$. Thus, $\Delta V_A(t) \leq 0$ can confirm that ι, Q_A, and λ_A satisfy the following inequalities:

$$\begin{aligned} Q_A &> \frac{1}{\iota}, \\ \lambda_A\mu_A\upsilon^2 - P_A - \iota P_A^2 F_A^2 &> 0 \end{aligned} \tag{21}$$

Since $V_A(t)$ is a nonnegative function and $\Delta V_A(t)$ is negative for sure, we can get the conclusion that when $t \to \infty$, $V_A(t) \to 0$. It is a signal where, for all k, $e_e(t)$ and $\widetilde{\Phi}(t)$ are bounded, and $\lim_{t\to\infty} e_e(t) = 0$.

From (13), we get the true value of the system output as follows:

$$x(t+1) = \hat{x}(t) + Z^T(t)\,\widehat{\Phi}(t) + Me_e(t) + e_e(t+1) \tag{22}$$

It is worth noting that $e_e(t+1)$ is unknown in time t. So, we transfer $e_e(t+1)$ into the following expression by two-step estimation technique:

$$e_e(t+1) \approx 2e_e(t) - e_e(t-1) \tag{23}$$

Therefore, (22) can be rewritten as

$$\begin{aligned} x(t+1) &= \hat{x}(t) + Z^T(t)\,\widehat{\Phi}(t) + (2-M)\,e_e(t) \\ &\quad - e_e(t-1) \end{aligned} \tag{24}$$

□

Remark 6. In order to make the parameter estimation law (15) have a strong capability in tracing time-varying parameters, a reset scheme should be considered as follows [17]:

$$\widehat{\Phi}(t) = \widehat{\Phi}(1), \quad \text{if } \widehat{\Phi}^T(t)\,\widehat{\Phi}(t) \leq \vartheta \text{ or } \hat{\theta}_1(t) \leq \vartheta, \tag{25}$$

where ϑ is a tiny positive constant and $\widehat{\Phi}(1)$ is the original value of $\widehat{\Phi}(t)$.

3.2. Model-Free Adaptive SMC Design and Stability Analysis. In order to eliminate the output non-following problem produced by the actuator saturation, an integral SMC based on antiwindup compensator is proposed [28]. Define the velocity tracking error as

$$e(t) = v^*(t) - v(t) - \xi(t), \tag{26}$$

where $v^*(t)$ means the given velocity reference value and $\xi(t)$ is the compensator signal which will be given later. To design the SMC, we choose an integral sliding surface as

$$s(t) = e(t) + \psi \sum_{i=1}^{t} T_s e(i), \tag{27}$$

where $\psi > 0$ and T_s denotes the sampling time of the control system. The closed-loop system stability can be guaranteed according to the following theorem.

Theorem 7. *When the integral sliding-mode surface is bounded, the tracking error of the control system is bounded, too. More specifically, for $|s(t)| \le \Omega$, the tracking error is bounded to a region as $\lim_{t\to\infty}|e(t)| \le 2\Omega/\psi T_s$.*

Proof. According to (27), we get

$$\begin{aligned} |e(t+1)| &= \frac{|e(t)|}{1+\psi T_s} + \frac{|s(t+1) - s(t)|}{1+\psi T_s} \\ &\le \frac{1}{1+\psi T_s}|e(t)| \\ &\quad + \frac{1}{1+\psi T_s}(|s(t+1)| + |s(t)|) \\ &\le \frac{1}{1+\psi T_s}|e(t)| + \frac{2\Omega}{1+\psi T_s} \end{aligned} \tag{28}$$

Due to the fact that $0 < 1/(1+\psi T_s) < 1$ and $2\Omega/(1+\psi T_s)$ is bounded, according to the stability criteria in [29], the tracking error can be bounded as

$$\lim_{t\to\infty} |e(t)| \le \frac{2\Omega}{\psi T_s} \tag{29}$$

The SMC law of the LIM can be designed based on observer (24) as

$$\begin{aligned} u^s(t) &= u(t-1) + u_f(t) + u_e(t) \\ u(t) &= \mathrm{Sat}\left\{\left(u(t-1)\right.\right. \\ &\quad + \mathrm{Sat}\left\{\left(u^s(t) - u(t-1)\right), T_s\dot{u}_{sq\min}, T_s\dot{u}_{sq\max}\right\}\Big), \\ &\quad \left.\left. T_s u_{sq\min}, T_s u_{sq\max}\right\}, \end{aligned} \tag{30}$$

where $u_f(t)$ and $u_e(t)$ denote the feedback and equivalent laws and $u^s(t)$ and $u(t)$ denote the primary and actual control input signals, respectively. And Sat$(\cdot)$ function is defined as

$$\mathrm{Sat}(h, h_{\min}, h_{\max}) = \begin{cases} h_{\max} & h \ge h_{\max} \\ h & h_{\max} > h > h_{\min} \\ h_{\min} & h_{\min} \ge h, \end{cases} \tag{31}$$

where $h_{\max}$ and $h_{\min}$ mean the upper and lower bound of Sat$(\cdot)$. One important thing is that when the input signal is within saturation, the tracking performance cannot be guaranteed. Thus, we design an antiwindup compensator signal as follows:

$$\xi(t) = \gamma\xi(t-1) + \widehat{\theta}_1(t)\left(u^s(t) - u(t-1)\right), \tag{32}$$

where γ is chosen in the unit disk. □

Remark 8. Since γ lies in the unit disk and assuming $u^s(t) - u(t-1)$ is bounded, the signal $\xi(t)$ is uniformly ultimately bounded (UUB) for all t according to [28].

Moreover, we concretely give the expressions of $u_f(t)$ and $u_e(t)$ as

$$\begin{aligned} u_f(t) &= -\frac{\widehat{\theta}_2(t) K_s s(t)}{\left(\widehat{\theta}_2^2(t) + \kappa\right)\left(1+\psi T_s\right)} \\ u_e(t) &= \frac{\widehat{\theta}_2(t)}{\widehat{\theta}_2^2(t) + \kappa}\Bigg(x^*(t+1) - \widehat{\theta}_1(t)\Delta d(t) - \widehat{x}(t) \\ &\quad - (2-M)e_e(t) + e_e(t-1) - \frac{e(t)}{1+\psi T_s} - \gamma\xi(t)\Bigg), \end{aligned} \tag{33}$$

where κ is also chosen in the unit disk, K_s is a negative constant chosen by $K_s^2/2 + K_s < 0$, and $x^*(t+1)$ means the reference signal value in time $t+1$.

Theorem 9. *For given $|\Delta x^*(t) - \Delta x^*(t-1)| \le \Delta x^*$, using control laws (31)–(33), the velocity tracking error of the LIM is UUB for all t with ultimate bound as $\lim_{t\to\infty}|e(t)| \le (q_1(t) + \sqrt{q_1^2(t) + 4q_0(t)q_2(t)})/q_0(t)\psi T_s$.*

Here, q_0 is a constant given by $q_0(t) \le -(K_s^2/2 + K_s)$, and

$$\begin{aligned} q_1(t) &= \frac{\kappa\left(K_s+1\right)\left(1+\psi T_s\right)q(t)}{\widehat{\theta}_1^2(t) + \kappa} \\ q_2(t) &= \frac{\kappa^2\left(1+\psi T_s\right)^2 q^2(t)}{2\left(\widehat{\theta}_1^2(t) + \kappa\right)} \\ q(t) &= -\frac{K_s s(t)}{1+\psi T_s} + x^*(t+1) - \widehat{\theta}_2(t)\Delta d(t) - \widehat{x}(t) \\ &\quad - (2-M)e_e(t) + e_e(t-1) - \frac{e(t)}{1+\psi T_s} \\ &\quad - \gamma\xi(t) \end{aligned} \tag{34}$$

Proof. Define the Lyapunov function $V_B(t) = (1/2)s^2(t)$; then, the difference of $V_B(t)$ can be figured by

$$\begin{aligned} \Delta V_B(t+1) &= V_B(t+1) - V_B(t) \\ &= \Delta s(t+1)\left[\frac{1}{2}\Delta s(t+1) + s(t)\right], \end{aligned} \tag{35}$$

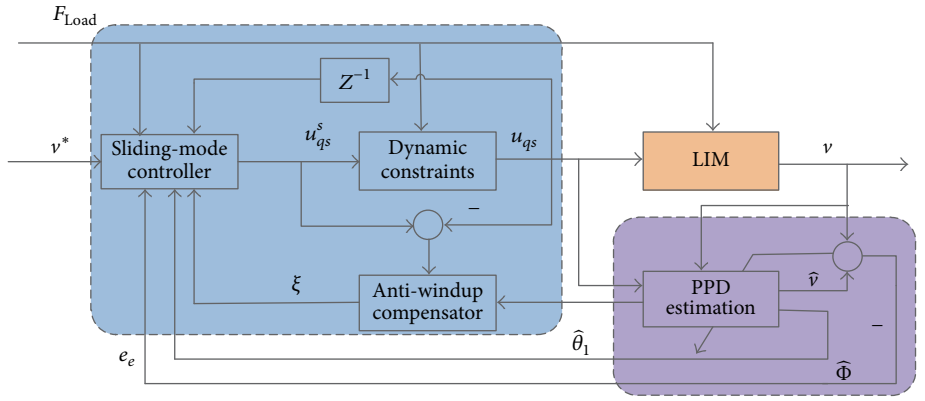

Figure 2: Diagram of LIM control systems.

where $\Delta s(t+1)$ is figured by

$$\begin{aligned}
\Delta s(t+1) &= s(t+1) - s(t) = (1+\psi T_s)\, e(t+1) \\
&- e(t) = (1+\psi T_s)\left(x^*(t+1) - \hat{x}(t)\right) \\
&- (2-M)\, e_e(t) - \hat{\Phi}(t)\, Z(t) + e_e(t-1) \\
&- \xi(t+1)\Big) - e(t) = (1+\psi T_s)\left(x^*(t+1) - \hat{x}(t)\right) \\
&- (2-M)\, e_e(t) + e_e(t-1) - \gamma\xi(t) - \hat{\theta}_2(t)\,\Delta d(t) \\
&- \hat{\theta}_1(t)\left(u_f(t) + u_e(t)\right)\Big) - e(t) = K_s s(t) \\
&+ \frac{\kappa(1+\psi T_s)}{\hat{\theta}_1^2(t) + \kappa}\left(-\frac{K_s s(t)}{1+\psi T_s} - \hat{x}(t) - \hat{\theta}_2(t)\,\Delta d(t)\right. \\
&+ x^*(t+1) - (2-M)\, e_e(t) + e_e(t-1) - \frac{e(t)}{1+\psi T_s} \\
&\left. - \gamma\xi(t)\right) = K_s s(t) + \frac{\kappa(1+\psi T_s)}{\hat{\theta}_1^2(t) + \kappa} q(t)
\end{aligned} \tag{36}$$

Besides, referring to (33), then we get

$$\begin{aligned}
\Delta V(t+1) &= \left(\frac{1}{2}K_s^2 + K_s\right) s^2(t) \\
&+ \frac{\kappa^2(1+\psi T_s)^2 q^2(t)}{2\left(\hat{\theta}_1^2(t) + \kappa\right)} \\
&+ \frac{\kappa(K_s+1)(1+\psi T_s)\, q(t)}{\hat{\theta}_1^2(t) + \kappa} s(t) \\
&\le -q_0(t)\, s^2(t) + q_1(t)\, s(t) + q_2(t),
\end{aligned} \tag{37}$$

where K_s is chosen to make $K_s^2/2 + K_s < 0$, and then $q_0(t) > 0$ is for sure. And when $s(t) > (q_1 + \sqrt{q_1^2 + 4q_0q_2})/2q_0$, $\Delta V(t+1) < 0$ can be guaranteed. Hence, the sliding surface is bounded as $\lim_{t\to\infty}|s(t)| \le (q_1 + \sqrt{q_1^2 + 4q_0q_2})/2q_0$. Finally, according to Theorem 9, we can get the conclusion that

$$\lim_{t\to\infty}|e(t)| \le \frac{\left(q_1 + \sqrt{q_1^2 + 4q_0q_2}\right)}{q_0\psi T_s} \tag{38}$$

□

Remark 10. Because ψ and κ are tiny positive constants, respectively, the ultimate bound of tracking error is 0; i.e., $\lim_{t\to\infty}|e(t)| = 0$.

Table 1: Parameters of LIM.

Parameters	Representation	Value
R_s (Ω)	Primary phase resistance	6.2689
R_r (Ω)	Secondary phase resistance	3.784
L_m (H)	Mutual inductance	0.0825
L_r (H)	Secondary phase inductance	0.1021
L_s (H)	Primary phase inductance	0.1021
M (kg)	Total mass of the object	3.25
D (kg/s)	Viscosity coefficient	40.95
h (m)	Polar distance	0.057

4. Simulation Results

In this section, a few simulation examples are given to testify the effectiveness of the designed controller compared to the classical PID controller. First of all, to clearly understand the control process of the LIM, a block diagram is given in Figure 2. Meanwhile, the parameters of the LIM are given in Table 1.

In order to obtain a satisfactory control effect, we choose the parameters of the controller as $N = 0.99$, $\vartheta = 300$, $\Phi(1) = [0.012, 0.005]^T$, $K_s = -1.5$, $\kappa = 0.0001$, $\psi = 10000$, $T_s = 0.001$, and $\gamma = 0.3$. Meanwhile, the parameters of the PID controller are $P = 300$, $I = 10000$, and $D = 0.1$. Two kinds of simulation experiments below are designed to prove the effectiveness of the proposed controller in this paper. By comparing the proposed controller with the PID

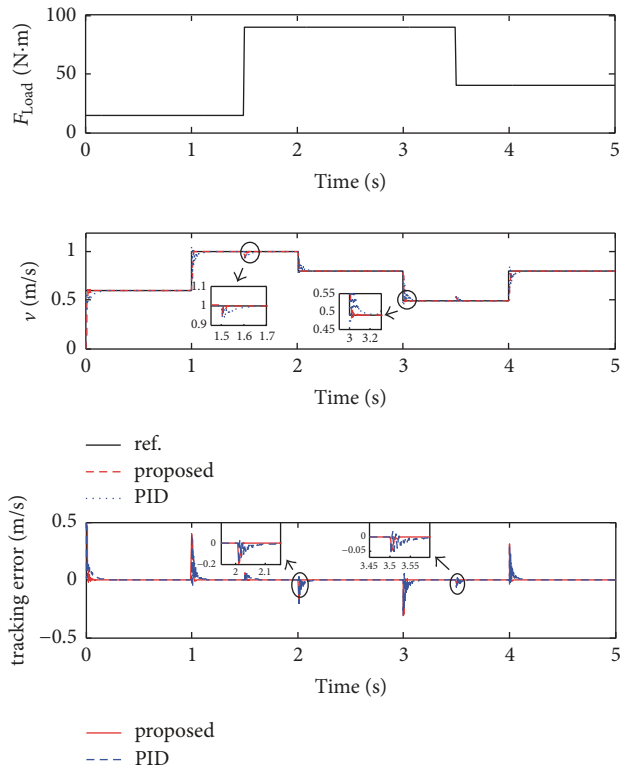

Figure 3: The reference tracking and tracking error curve of the proposed controller and PID controller (step signal).

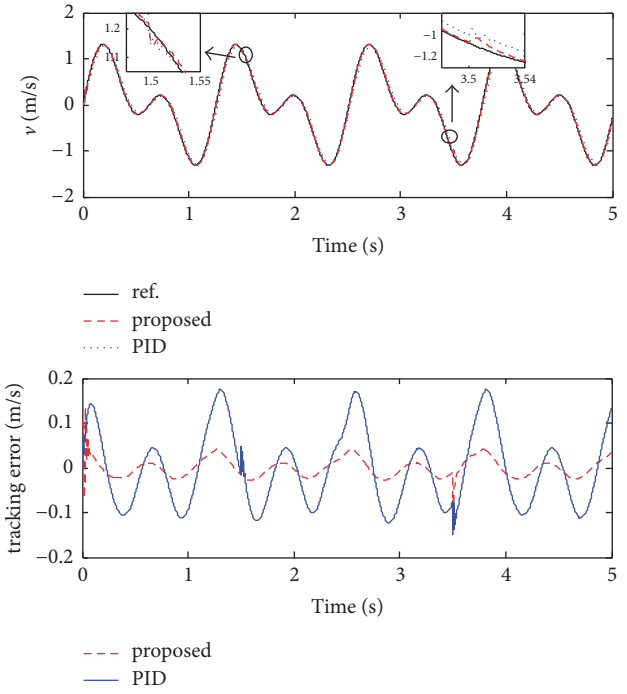

Figure 4: The reference tracking and tracking error curve of the proposed controller and PID controller (periodic signal).

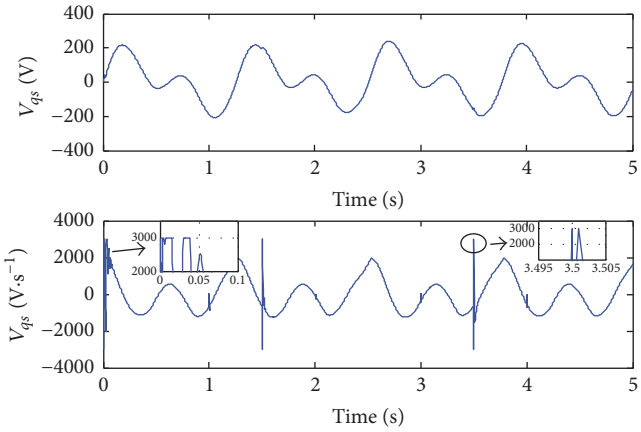

Figure 5: The value of input signals (periodic signal).

controller, we will analyze the control performance from the following aspects: dynamic performance, static performance, anti-interference, and robustness.

(1) To test the tracking performance and anti-interference, we select the step signal and time-varying periodic signal as our given velocity reference, respectively. Meanwhile, the load torque changes as shown in Figure 3. The velocity tracking performance and tracking error are also shown in Figures 3 and 4. As the figures show, it can be clearly known that both controllers can ensure that there is no steady-state error at steady state for step signal. However, the proposed control method enables the control system to enter steady state faster within 0.12 s (within is 0.3 s for the PID controller). Besides, when the load torque changes at 1.5 s and 3.5 s, the speed of the LIM under the proposed controller is still able to track the given signal quickly within 0.1 s after a small fluctuation (within 0.32 s for the PID controller). It can be seen more prominently in Figure 4 that the proposed controller can make the system output track the time-varying periodic signal perfectly with less than 0.05 m/s error. The input signal under time-varying periodic signal is shown in Figure 5. The compensator signal under time-varying periodic signal is shown in Figure 6. From Figures 5 and 6, we can get the information that, by adding the antiwindup compensator, the control system can quickly exit from saturation but still trace the reference quite well. The values of the PPDs are shown in Figure 7.

(2) To test the robustness of the proposed controller, we increase the mover mass to three times and five times the original, and this simulation is also under time-varying periodic signal. The tracking performance is shown in Figure 8. From Figure 8, we know that no matter how the mover mass changes, the speed of the LIM can always follow the given reference satisfactorily, and that is another merit of the model-free adaptive sliding-mode-constrained controller. Therefore, this simulation verifies the robustness of the proposed controller.

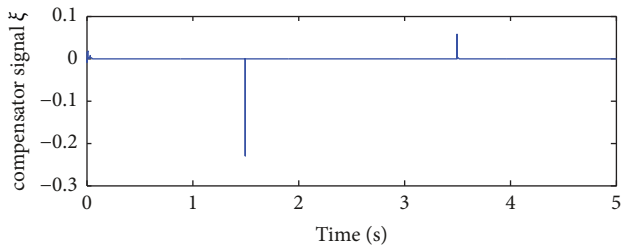

Figure 6: The value of compensator signals (periodic signal).

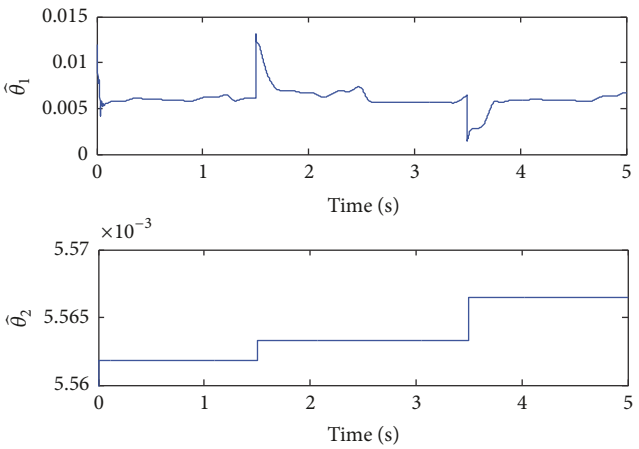

Figure 7: The value of PPDs (periodic signal).

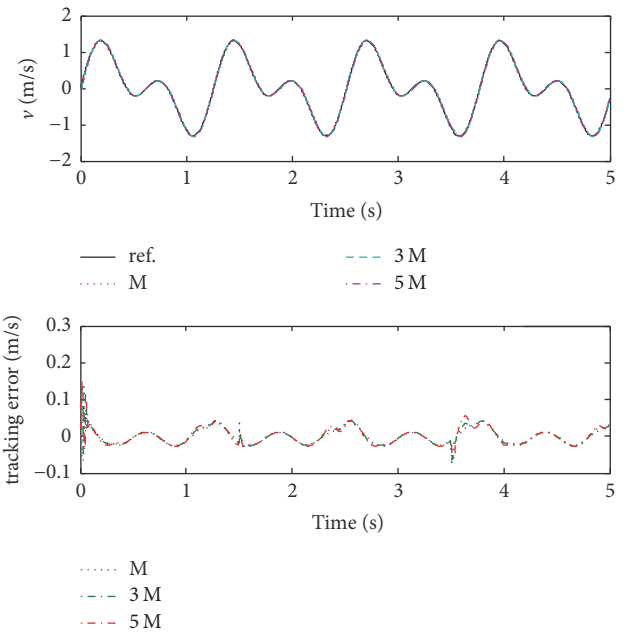

Figure 8: Velocity tracking curve under different mover mass (periodic signal).

5. Conclusion

In this paper, a model-free adaptive sliding-mode controller is proposed to deal with the problem of the speed tracking of the LIM considering end effects. First of all, the CFDL technique is applied to linearize the LIM model which has been transferred into a NARX form. Then, the controller is designed based on PPD estimation algorithm. Through the process of designing, an antiwindup compensator is designed to handle the problem of input saturation. Lyapunov stability theory proves the stability of the closed-loop system theoretically, and the simulation results verify the effectiveness of the proposed method to the LIM system.

Data Availability

All the underlying data related to this article are available upon request.

Conflicts of Interest

The authors declare that there are no conflicts of interest regarding the publication of this paper.

Acknowledgments

This work was partially supported by the National Natural Science Foundation of China (61503156, 61403161, and 61473250) and the National Key Research and Development Program (2016YFD0400300).

References

[1] M. H. Ravanji and Z. Nasiri-Gheidari, "Design Optimization of a Ladder Secondary Single-Sided Linear Induction Motor for Improved Performance," *IEEE Transactions on Energy Conversion*, vol. 30, no. 4, pp. 1595–1603, 2015.

[2] X. Qiwei, S. Cui, Q. Zhang, L. Song, and X. Li, "Research on a new accurate thrust control strategy for linear induction motor," *IEEE Transactions on Plasma Sciences*, vol. 43, no. 5, pp. 1321–1325, 2015.

[3] H. Gurol, "General atomics linear motor applications: Moving towards deployment," *Proceedings of the IEEE*, vol. 97, no. 11, pp. 1864–1871, 2009.

[4] S. E. Abdollahi, M. Mirzayee, and M. Mirsalim, "Design and Analysis of a Double-Sided Linear Induction Motor for Transportation," *IEEE Transactions on Magnetics*, vol. 51, no. 7, 2015.

[5] A. Boucheta, I. K. Bousserhane, A. Hazzab, P. Sicard, and M. K. Fellah, "Speed control of linear induction motor using sliding mode controller considering the end effects," *Journal of Electrical Engineering & Technology*, vol. 7, no. 1, pp. 34–45, 2012.

[6] I. Boldea and S. A. Nasar, "Linear electric actuators and generators," *IEEE Transactions on Energy Conversion*, vol. 14, no. 3, pp. 712–717, 1999.

[7] A. Accetta, M. Cirrincione, M. Pucci, and G. Vitale, "Neural sensorless control of linear induction motors by a full-order luenberger observer considering the end effects," *IEEE Transactions on Industry Applications*, vol. 50, no. 3, pp. 1891–1904, 2014.

[8] G. Kang and K. Nam, "Field-oriented control scheme for linear induction motor with the end effect," *IEE Proceeding—Electrical Power Applications*, vol. 152, no. 6, pp. 1565–1572, 2005.

[9] F. E. Benmohamed, I. K. Bousserhane, A. Kechich, B. Bessaih, and A. Boucheta, "New MRAS secondary time constant tuning for vector control of linear induction motor considering the end-effects," *COMPEL - The International Journal for Computation and Mathematics in Electrical and Electronic Engineering*, vol. 35, no. 5, pp. 1685–1723, 2016.

[10] A. Boucheta, I. K. Bousserhane, A. Hazzab, B. Mazari, and M. K. Fellah, "Adaptive backstepping controller for linear induction motor position control," *COMPEL: The International Journal for Computation and Mathematics in Electrical and Electronic Engineering*, vol. 29, no. 3, pp. 789–810, 2010.

[11] H.-H. Chiang, K.-C. Hsu, and I.-H. Li, "Optimized adaptive motion control through an SoPC implementation for linear induction motor drives," *IEEE/ASME Transactions on Mechatronics*, vol. 20, no. 1, pp. 348–360, 2015.

[12] F. Alonge, M. Cirrincione, M. Pucci, and A. Sferlazza, "Input-output feedback linearization control with on-line MRAS-based inductor resistance estimation of linear induction motors including the dynamic end effects," *IEEE Transactions on Industry Applications*, vol. 52, no. 1, pp. 254–266, 2016.

[13] A. Y. Alanis, J. D. Rios, J. Rivera, N. Arana-Daniel, and C. Lopez-Franco, "Real-time discrete neural control applied to a Linear Induction Motor," *Neurocomputing*, vol. 164, pp. 240–251, 2015.

[14] A. Boucheta, I. K. Bousserhane, A. Hazzab, B. Mazari, and M. K. Fellah, "Fuzzy-sliding mode controller for linear induction motor control," *Revue Roumaine Des Sciences Techniques - Serie Electrotechnique Et Energetique*, vol. 54, no. 4, pp. 405–414, 2009.

[15] C.-Y. Hung, P. Liu, and K.-Y. Lian, "Fuzzy virtual reference model sensorless tracking control for linear induction motors," *IEEE Transactions on Cybernetics*, vol. 43, no. 3, pp. 970–981, 2013.

[16] Z. Hou, *The parameter identification, adaptive control and model free learning adaptive control for nonlinear systems [Ph.D. thesis]*, Northeastern Univerity, Shenyang, 1994.

[17] Z.-S. Hou and S.-T. Jin, "A novel data-driven control approach for a class of discrete-time nonlinear systems," *IEEE Transactions on Control Systems Technology*, vol. 19, no. 6, pp. 1549–1558, 2011.

[18] Z. Hou and S. Jin, "Data-driven model-free adaptive control for a class of MIMO nonlinear discrete-time systems," *IEEE Transactions on Neural Networks and Learning Systems*, vol. 22, no. 12, pp. 2173–2188, 2011.

[19] D. Xu, B. Jiang, and P. Shi, "A novel model-free adaptive control design for multivariable industrial processes," *IEEE Transactions on Industrial Electronics*, vol. 61, no. 11, pp. 6391–6398, 2014.

[20] X. Bu, Z. Hou, and H. Zhang, "Data-Driven Multiagent Systems Consensus Tracking Using Model Free Adaptive Control," *IEEE Transactions on Neural Networks Learning Systems*, vol. PP, no. 99, p. 11, 2017.

[21] D. Xu, B. Jiang, and P. Shi, "Adaptive observer based data-driven control for nonlinear discrete-time processes," *IEEE Transactions on Automation Science & Engineering*, vol. 11, no. 4, pp. 1549–1558, 2014.

[22] D. Xu, Y. Shi, and Z. Ji, "Model Free Adaptive Discrete-time Integral Sliding Mode Constrained Control for Autonomous 4WMV Parking Systems," *IEEE Transactions on Industrial Electronics*, 2017.

[23] Z. Wu, X. Wang, and X. Zhao, "Backstepping terminal sliding mode control of DFIG for maximal wind energy captured," *International Journal of Innovative Computing, Information and Control*, vol. 12, no. 5, pp. 1565–1579, 2016.

[24] X.-G. Yan and C. Edwards, "Adaptive sliding-mode-observer-based fault reconstruction for nonlinear systems with parametric uncertainties," *IEEE Transactions on Industrial Electronics*, vol. 55, no. 11, pp. 4029–4036, 2008.

[25] Z. Hou, W. Wang, and S. Jing, "Adaptive quasi-sliding-mode control for a class of nonlinear discretetime systems," *Control Theory Applications*, vol. 26, no. 5, pp. 505–509, 2009.

[26] Z.-S. Hou and Z. Wang, "From model-based control to data-driven control: survey, classification and perspective," *Information Sciences*, vol. 235, pp. 3–35, 2013.

[27] D. Xu, B. Jiang, and F. Liu, "Improved data driven model free adaptive constrained control for a solid oxide fuel cell," *IET Control Theory & Applications*, vol. 10, no. 12, pp. 1412–1419, 2016.

[28] N. Ji, D. Xu, and F. Liu, "A novel adaptive neural network constrained control for solid oxide fuel cells via dynamic anti-windup," *Neurocomputing*, vol. 214, pp. 134–142, 2016.

[29] J. Spooner, M. Maggiore, and K. Passino, *Stable adaptive control and estimation for nonlinear systems*, Wiley, New York, NY, USA.